Trans. Phenom. Nano Micro Scales, 3(2): 68-76, Summer - Autumn
DOI: 10.7508/tpnms.2015.02.001

ORIGINAL RESEARCH PAPER

Numerical Study on Low Reynolds Mixing of T-Shaped Micro-Mixers with Obstacles

M. R. Rasouli[1], A. Abouei Mehrizi[1], A. Lashkaripour[1,*]
[1] *Biomedical Engineering Division, Life Science Engineering Department, Faculty of New Sciences and Technologies, University of Tehran, Tehran, I.R. Iran.*

ARTICLE INFO.

Article history
Received 9 January 2015
Accepted 30 May 2015

Keywords
Grooved
Micromixers
Mixing Efficiency
Obstacle
T-shaped

Abstract

Micromixers are one of the most crucial components of Lab-On-a-Chip devices with the intention of mixing and dispersion of reagents like small molecules and particles. The challenge facing micromixers is typically insufficient mixing efficiency in basic designs, which results in longer microchannels. Therefore, it is desirable to increase mixing efficiency, in order to decrease mixing length, which enables miniaturization of Lab-On-Chip devices. This study investigates two different designs of a passive T-shaped micromixer employing several rectangular obstacles and grooves to monitor mixing efficiency with geometry change, while keeping the Reynolds number under 2. The mixing performance of these geometries is studied by numerical study and it was implemented in COMSOL Multiphysics environment. It was clarified that T-shaped micromixer with obstacles and grooved micromixer improved mixing efficiency of the basic design by 37.2% and 43.8%, respectively. Also, it was shown that this increase in mixing efficiency was due to the development of transversal component of flow caused by the obstacles and grooves.

1. Introduction

The development of microsystem technology and micromechanical systems has been trending in the global technological progress in the last few decades. Miniaturization is desirable, due to the possibility of performing complicated analysis in a handhold size device, with faster sample analysis, higher throughput, portability, and reduced reagent use, while keeping cost lower than macro devices [1]. Microfluidics holds promise for wide range of novel applications in the field of chemistry, biology and medicine [2]. Microfluidic devices have made a revolution within biomedical and biochemical sciences from last few years due to their broad applications in areas such as cell storing , DNA assay, proteins, high throughput screening, surface patterning of cells, and high throughput nucleic acid analysis, to name a few [3-5]. Mixing of fluids is an extremely crucial process in various microfluidic devices. To increase the rate of mixing, it is necessary to use special components such as micromixers [6]. A key component in microfluidic systems is the micromixer, whenever the mixing of fluids becomes critical, like in reagents such as small

[*]Corresponding author
Email address: a.lashkaripour@ut.ac.ir

Nomenclature

j	Diffusion (mol/s.m^2)	I	Identity matrix
c	Concentration of species (mol/m^3)	F	Force (N)
D	Diffusion coefficient (m^2/s)	μ	Viscosity (Pa.s)
f	Species mole fraction	L	Representative length (m)
u	Velocity (m/s)	R	Rate of change of concentration (mol/s.m^3)
ρ	Density (kg/m^3)	A	Cross section area (m^2)
		η	Mixing efficiency (%)

molecules, large macromolecules, and particles [7].The primary goal of a micromixer is to mix the reactants for initiation of the reaction process, which makes it an irreplaceable component in lab-on-a-chip (LOC) platforms in sophisticated chemical reactions. Micromixers are capable of integration in microfluidic systems or working as a singular device [8]. In practice, it brings a challenge to mix several fluids in micro-scale due to the low Reynolds number of flows in such dimensions (usually below 100) [9]. Mixing process in macro-flows is typically turbulent, however, micro-flows are usually laminar, and mixing under normal conditions is only a result of molecular diffusion [6]. In the microscopic flows convective mass transfer occurs only in the flow direction, therefore, diffusion alone is insufficient and inefficient, which means long microchannels are required in order to reach the mixing goal. This insufficiency imposes that mixing in micro-scale flows should be artificially enhanced [1]. Passive micromixers depend merely on enhancing mixing through lamination of the solute flow, in a pressure driven flow. Kumar et al. [10] demonstrated that the swaying of the fluids in microchannel with obstacles will result in chaotic advection, and an improved micromixing performance, consequentially. These transversal components of the flow field enhance mixing of different fluid components within length scales of the order of centimeters making it suitable for LOC applications [11].

Computational fluid dynamics (CFD) has been widely conducted to investigate and study the design and performance of micromixers [12-15]. The effects of operating and design parameters on mixing characteristics were studied by Gobby et al. [16]. It was shown that the mixing length increases with the fluid speed and it is also influenced by the mixer aspect ratio. Also, it was clarified that changing the angle between the inlet channels has not a significant effect on the mixing performance, on the other hand, throttling the fluid considerably decreases the mixing length. Engler and et al. investigated and improved the mixing quality in T-shaped mixers, using CFD method [17]. The effects of geometric parameters on mixing efficiency in a grooved micromixer was clarified by Yang and et al. [18]. It was illuminated that the depth ratio and asymmetry index are the dominant geometric parameters affecting mixing efficiency. Soleymani et al. [19] carried out a numerical and experimental investigations of liquid mixing in T-shaped micromixers. It was proven that the occurrence and the development of vortices in the entrance of a T-shaped micromixer were necessary for a satisfactory mixing performance. Shih et al. [20] simulated a planar micromixer with convection and diffusion over a wide range of Reynolds numbers. By the means of Taguchi design of experiment (DOE) method, they have succeeded in reaching a mixing efficiency of 85%. It was clarified mixing efficiency can be improved by placing a number of obstacles in mixing flow to change the flow field, therefore, enhancing mixing. In a laminar flow, a symmetrical arrangement of obstacles is inefficient. Besides, the characteristic size of the obstacles should be comparable to the channel size. It should be taken into consideration that the mixer could be optimized for this parameter [21]. Bhagat and et al. [22] simulated a micromixer with obstacles to study mixing at low Reynolds numbers. Their design was characterized by low pressure drop and a simple planar structure, with easy fabrication. In this paper we simulated a T-shaped micromixer and studied the influence of two different geometries with rectangular obstacles on the regarded micromixer's mixing efficiency. The rest of the paper is as follows. In Section 2, the geometries and parameters of simple, grooved and with obstacles T-shaped micromixer is given and its implementation in COMSOL version 4.4 is introduced. In section 3, the effects of grooves and obstacles on the concentration distribution along the channel and the

velocity distribution was investigated. Moreover, mixing efficiency of these three geometries were analyzed and compared. Finally, a comprehensive discussion concludes the paper.

2. Modeling

In this section, a basic design of a T-shaped micromixer will be introduced. Afterwards, two different set of obstacles will be added to the basic design in order to enhance the mixing efficiency. The following section will introduce the basic geometry, and the geometries of the two enhanced designs. Moreover, the modeling of the flow field will be discussed. Finally, the numerical method conducted in this study in order to solve the simulation will bring this section to an end.

2.1. Microchannel Geometry and Boundary Conditions

The basic geometry includes a straight microchannel with two inlets, for two different species, that form a T-shaped micro mixer. For species transport, a constant concentration condition is imposed at the channel inlets. Two fluid streams with different concentrations (c_0=1 and c_0=0) are assumed to flow into the upper and lower inlets with identical pressure potential that leads to same velocity along channel. This boundary condition can be prescribed as a Dirichlet condition for a P=P_0 pressure. Therefore, Dirichlet boundary conditions were used at flow inlet and outlet.

At the walls of microchannels, the boundary conditions for the fluid velocity components at walls are typically no-slip condition and zero flux condition is executed for the species, while convective-flux-only boundary condition is applied at the channel outlet and the normal gradients of pressure on the solid walls of the micromixer was considered to be zero. The described boundary conditions are also given in table 2.

Table 1
Boundary conditions implemented in model.

Setting	Boundary type	Boundary condition	p
Boundaries 1,2	Inlet	Pressure, No vicious stress	P_0=300 Pa
Boundaries 7	Outlet	Pressure, No vicious stress	P=0
All others	wall	No slip	-

The basic design that was considered for this study was based on Rudyak and Minakov work [6]. The width of the mixing channel is 100 µm; the width of the inlet channels is 50 µm, and the height of the mixer was assumed to be 50 µm. Figure 1a shows the basic geometry of the T-shaped micromixer that was used in this paper.

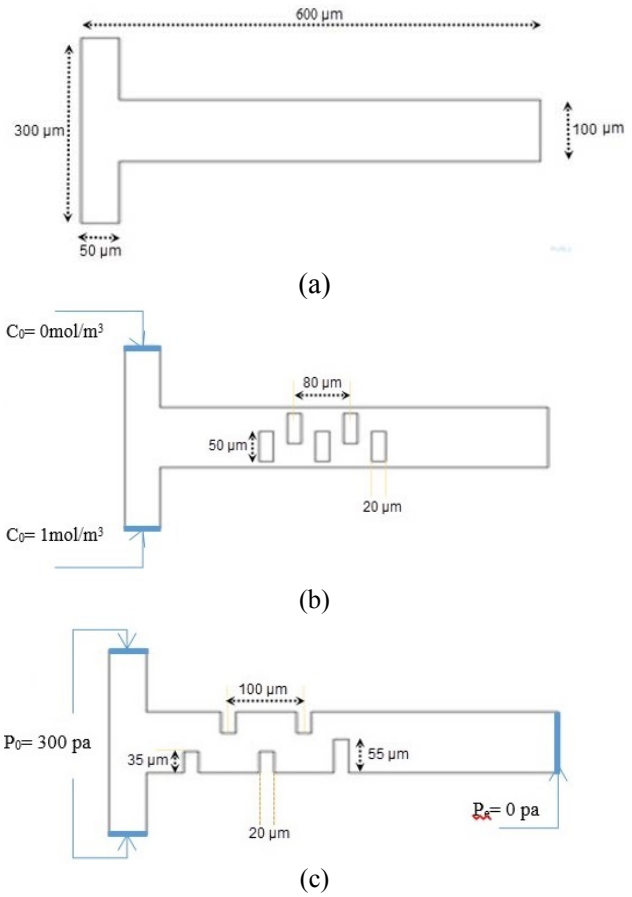

Fig. 1. Mixing Geometry of two fluids, in (a) the basic T-shaped mixer (b) T-shaped micromixer with obstacles and (c) grooved T-shaped micromixer

2.1.1. T-shaped micromixer with obstacles

A two-dimensional microchannel domain with 5 obstacles in middle of surface is considered as the computational domain for the first optimized design. Obstacles have a width of 20 µm and a height of 50. The gap between each obstacles is 50 µm and a 5 µm gap between obstacles and the channel walls was embedded.

Figure 1b illustrates the geometry of this T-shaped micromixer.

2.1.2. Grooved T-shaped micromixer

A two-dimensional microchannel domain with grooves at the surface, is considered as the computational domain for the second optimized design. Grooves have a width of 20 μm and height of 35 μm except for the last groove that the height was induce by 20 μm to that of formers. The gap between each groove is considered to be 55 μm (2.5 times of obstacles width). Microchannel with asymmetric geometry evidenced to have higher efficiency according to literature. Hence we arranged obstacles completely asymmetric. The geometry of this micromixer is shown in figure 1c.

2.2. Flow Field Modeling

In this analysis, fluids are assumed to be incompressible, laminar, miscible liquid flows with uniform properties, as well as negligible effects of gravity and temperature variation over the computational domain. These assumptions are typical of a microfluidic flow. As mentioned in the literature, diffusion plays a crucial rule in the mixing process. Diffusion is defined as the Process of spreading molecules from a region of higher concentration to the region of lower concentration by Brownian motion, which results in a gradual mixing of materials. In this study diffusion was described mathematically according to Fick's law:

$$j = -D\frac{dc}{dx} \tag{1}$$

Where c is the species concentration, x is the position of the species along the channel, and D is the diffusion coefficient. For simple spherical particles [23]. In this simulation, the temperature variations in the flow was considered to be negligible. Under such condition a single-phase fluid can often assumed to be incompressible; which results in a constant density (ρ).

This is the case for all liquids under normal conditions and also for gases at low velocities. For a constant density equation 2 and equation 3 can be given.

$$\rho\nabla.u = 0 \tag{2}$$

$$\rho\frac{\partial u}{\partial t} + \rho(u.\nabla)u = \nabla.[-pI + \mu(\nabla u + (\nabla u)^T)]+F \tag{3}$$

Fundamental to the analysis of fluid flow is the Reynolds number:

$$Re = \frac{\rho UL}{\mu} \tag{4}$$

Where U denotes a velocity scale, μ is the dynamic viscosity and L denotes a representative length. The Reynolds number represents the ratio between inertial and viscous forces. At low Reynolds numbers, viscous forces dominate and tend to damp out all disturbances, which leads to a laminar flow, which was correctly assumed in this study. This analysis was aimed to monitor the concentration distribution of the two inlet fluids. These flows are considered to have a same viscosity at different geometric conditions. These fluids undergo mixing through convective and diffusive transport. The species transport for an incompressible flow is governed by equation 5 [24-25].

$$\frac{\partial c}{\partial t} + u_x\frac{\partial c}{\partial x} + u_y\frac{\partial c}{\partial y} + u_z\frac{\partial c}{\partial z} = D\left[\frac{\partial^2 c}{\partial x^2} + \frac{\partial^2 c}{\partial y^2} + \frac{\partial^2 c}{\partial z^2}\right] + R \tag{5}$$

As mentioned before, c is the species concentration of the fluid, u_x, u_y and u_z, are the velocity components in x, y and z direction, respectively. The solution for the velocity field is determined independently by solving the Navier–Stokes equations for a given geometry.

Consequently, this solution is used to solve the steady state convection-diffusion equation. D is the diffusion coefficient and R is the rate of change of concentration of fluid produced by chemical reaction. In this paper flow is assumed to be steady state, non-reactive and fully developed, because of these assumptions equation 5 could be reduced to:

$$u_z\frac{\partial c}{\partial z} = D\left[\frac{\partial^2 c}{\partial x^2} + \frac{\partial^2 c}{\partial y^2}\right] \tag{6}$$

Since this paper considers only incompressible flows and the equations of motion contain only the pressure gradient, therefore, there is no need to calculate the absolute pressure. As a result in this study, the relative pressure is used to simulate the flow. The parameters that were necessary to solve the numerical simulation are given in table 3.

Table 3
Parameters implemented in the simulation.

Description	Expression	Name
ρ	1.e3 [kg/m^3]	Density
η	1.e-3 [Pa.s]	Viscosity
D	5e-9 [m^2/s]	Diffusion Constant
C_0	0 [mol/m^3]	Inlet Concentration of (A)
C_1	1 [mol/m^3]	Inlet Concentration of (B)

2.3. Numerical setup

If convection-diffusion equations are discretized using the Galerkin finite element method, the solution will become unstable.

Stabilized finite element methods are therefore necessary to gain a converging solution. At very low diffusion coefficients convective term feed the numerical solution with energy, which does not only move the solution but also other small random fluctuations which are generally small, but when convective term feeds the solution with energy, they become large and destabilize the numerical solution. Therefore, in order to stabilize the CFD solution at low diffusion coefficients, artificial diffusion concept was used.

2.4. Mesh Verification Analysis

The Grid Convergence Index (GCI) methodology [26] was exploited to estimate discretization error and mesh verification purposes. The GCI was applied at three levels of mesh density (fine, extra fine and extremely fine) in order to evaluate the order of convergence (Table 4).

Table 4
Element meshes.

Mesh	Number of elements	Mixing Efficiency	GCI
Extremely Fine	28791	61.485%	0.37%
Extra Fine	23999	61.62%	
Fine	9016	62.08%	

The rate of convergence is computed on mixing efficiency at the outlet of micromixer. The GCI for the grids is less than 0.3%.

3. Results and Discussion

In this study, velocity distribution, concentration distribution and mixing efficiency of the basic T-shaped micromixer and the two optimized designs will be investigated and compared. The output of the simulations are given as follows.

3.1. Velocity distribution

For all three geometry Reynolds number remains under 2 (1.7-1.9); hence the flow field is strongly dependent on the channel geometry, specifically the obstacles that the flow bumps into significantly alters the flow field. The velocity distribution in the basic and two enhanced geometries are illustrated in figure 2-4.

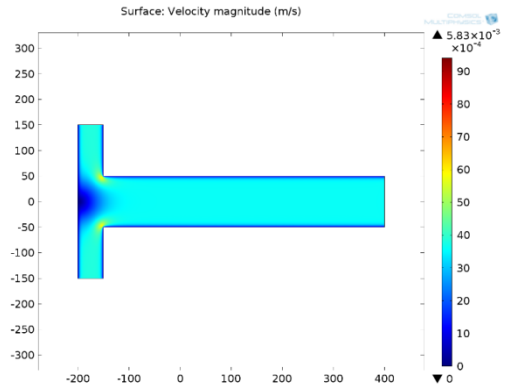

Fig. 2. Velocity distribution in plain T-shaped micro mixer

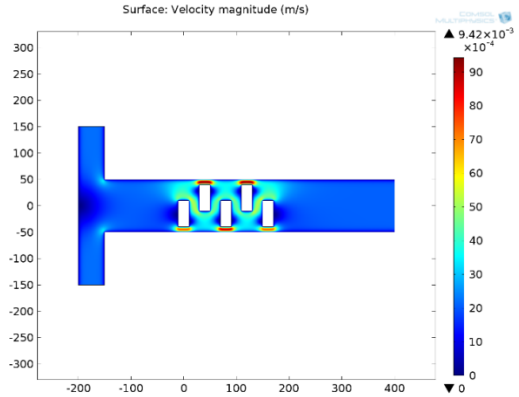

Fig. 3. Velocity distribution in T-shaped micromixer with obstacles

It is clear that significant mixing in passive micromixers takes place through diffusion, as a result insertion of obstacles in micromixers will break up the flow with the velocity induced in the transverse direction. This phenomena will enhance the efficiency of mixing in given channels and therefore the mixing length will be decreased, which is essential for mixing enhancement. It should be added that the mixing between the two flows occurs mainly in the narrow

channel after they collided with the obstacle producing the turbulence. The added effect of setting boundary protrusion can also facilitate stirring of the fluids near the channel sidewalls to achieve a better mixing**.** It is anticipated that presence of obstacles will generate vortex around the blocks, this circumstance also led to follow-on transverse velocity component which is desirable outcome to enhance mixing. The results for velocity field that are depicted in figure 4-6 suggest that the geometry with grooves on the wall develop transverse velocity component further compared to other geometries.

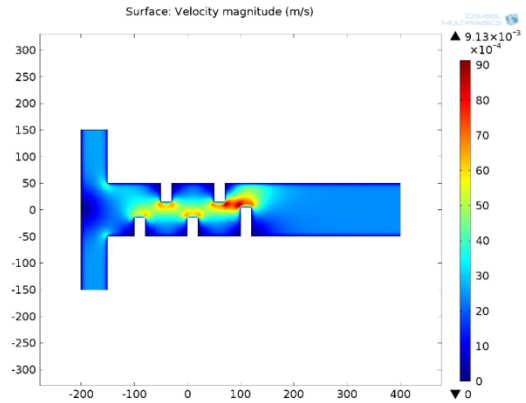

Fig. 4. Velocity distribution in grooved T-shaped micro mixer

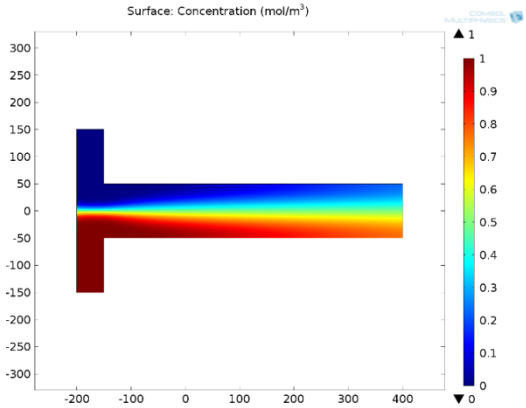

Fig. 5. Concentration distribution in plain T-shaped micro mixer

3.2. Concentration distribution

In the previous section, field velocity for all geometries were illustrated and discussed. Since there is no obstacle in fluid path in basic geometry and flow is completely laminar (owing to low Reynolds number) it can be observed that no velocity component in y direction was developed. As a result, the molecular flux is purely diffusive with no contribution from convection, as shown in figure 5. In the absence of transversal components in the flow fields the mixing is limited to the initial interface between the two flows. This results in comparatively longer mixing path in comparison to two enhanced designs.

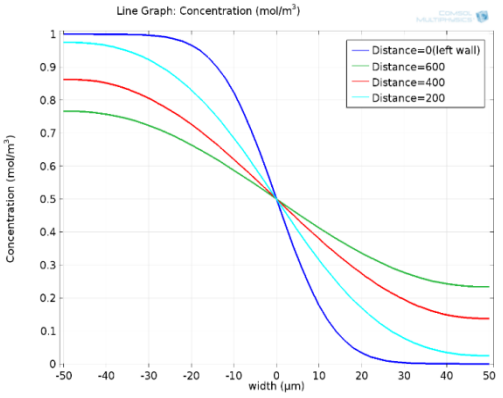

Fig. 6. Concentration change in several cross sections with respect channel width in basic micro mixer

The variation of concentration with respect to channel with in four cross sections along the basic micromixer had been illustrated in figure 6. As it is expected the variation of concentration starts from 0-1 at the left wall where no mixing has occurred yet. In the distance of 600 µm this variation decreases to about 0.22-0.77, which shows although mixing has taken place, it is not sufficient for a favorable mixing.

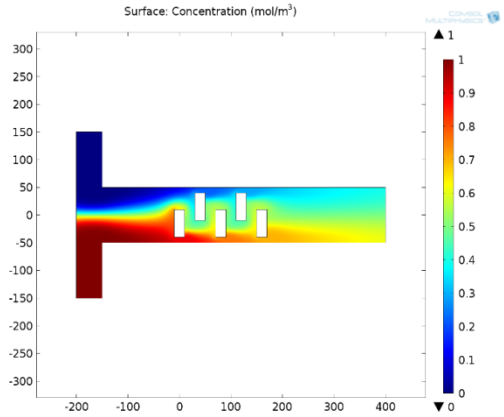

Fig. 7. Concentration distribution in T-shaped micromixer with obstacles

Nevertheless, in designs employing surface patterns, the mixing was greatly enhanced. This improvement is due to the convective effects associated with the transversal flows generated by the asymmetric obstacles as shown in figure 7 and figure 9. As

expected, in micromixer with obstacles concentrate distribution at the exit is more uniform. This is mainly due to transverse component formed by bumping to obstacles as described earlier.

Figure 8, shows the variation of concentration in different cross sections along the micromixer. As before, it has started from 0-1 and decreased to reach its minima of 0.4-0.6. A comparison of figure 6 and figure 8 reveals mixing has significantly enhanced in respect to basic design.

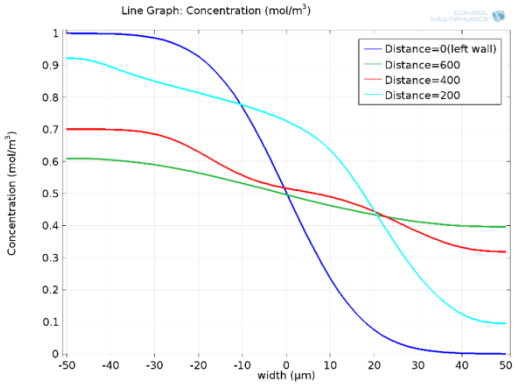

Fig. 8. Concentration change in several cross sections with respect channel width in micromixer with obstacles

In the second optimized geometry, the arrangement of grooves cause stretching and folding of flow this procedure extends contact surface and as a result diffusion increases. As pointed out previously this will result in an enhanced mixing efficiency. Figure 9 demonstrates concentration distribution for this geometry it implies more uniform concentration at the exit for grooved geometry. Figure 10 illustrates the concentration change in several cross sections with respect channel width. As it is clear the variation of concentration in cross section closer to inlet is close 0 to 1, however, this variation becomes smaller along the microchannel with the increase of length. Also, it could be seen this variation becomes negligible at the inlet (less than 0.4-0.58). Therefore, grooved micromixer not only shows a more desirable mixing performance, but also exceeds the performance of micromixer with obstacles.

To evaluate performance of these three micromixers that have been investigated more accurately, a measure called mixing index will be used.

3.3. Mixing Efficiency Evaluation

As mentioned earlier, during the mixing event, the species concentration on one side of the channel will be reduced from 1, while on the other side it will increase from 0.

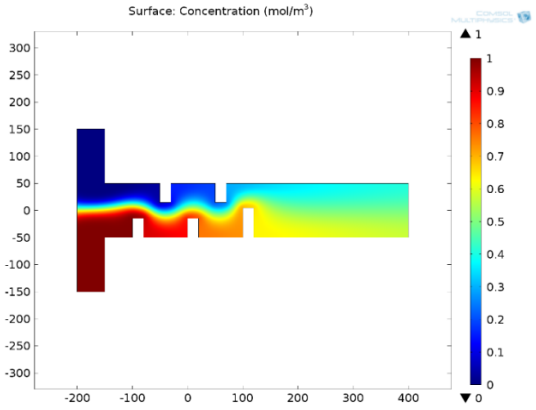

Fig. 9. Concentration distribution in grooved T-shaped micromixer

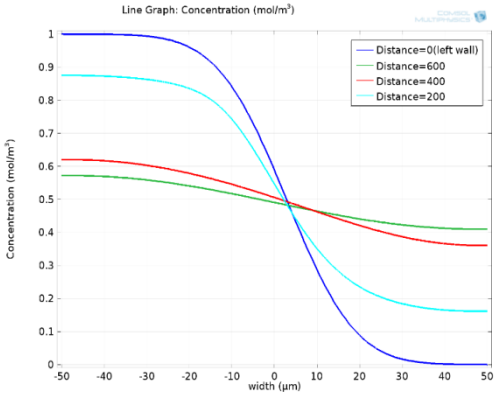

Fig. 10. Concentration change in several cross sections with respect channel width in grooved micro mixer

The mixing performance is typically evaluated by quantifying the deviation from the perfectly mixed state, [27], as shown in equation 7. For uniform mixing, the deviation of the concentration should be 0 with a mixing index of 1. Conversely, as the mixing index decreases from 1, a lesser amount of mixing is accomplished.

$$\eta = \left[1 - \frac{\sqrt{{}^{1}/_{N}\sum_{1}^{N}(\bar{c} - \bar{c}^{*})^{2}}}{\sqrt{{}^{1}/_{N}\sum_{1}^{N}(\bar{c}^{0} - \bar{c}^{*})^{2}}}\right] \quad (7)$$

In equation 7, N is the number of points in the cross section used for estimation of the mixing index. The variable c represents the scaled concentration value at that point, while c_0 and c^* are the scaled concentration

at each point if the solutions are unmixed and the concentration with perfect mixing (i.e.,0.5), respectively. Also, it should be noted that the variable c_0 takes on a value of 0 or 1 at any point across the channel cross section, resulting in a constant denominator value of 0.5 in equation 7. In this study, an integral form of the equation 7 is used to estimate the mixing performance as shown in equation 8. The mixing indexes are calculated based on the sampling of the concentration profile at exit.

$$\eta = \left[1 - 2 * \sqrt{\frac{\int_A (\bar{c} - \bar{c}^*)^2 \, dA}{\int_A dA}}\right] \quad (8)$$

Therefore, η=0 indicates a completely unmixed state, and η=1 indicates complete mixing. In equation 8, A is the cross section area at which the mixing index is calculated. The cross section area A is variable due to the presence of grooves at the bottom surface. In this paper we evaluated mixing index for exit boundary so A is the height of channel. Table 5 summarizes the results of the mixing index for all three geometries, also the increase in percentage of mixing efficiency is given.

Table 5
Mixing efficiency of micromixers with different designs.

Mixer	Plain	With Obstacles	Grooved
Mixing Efficiency	61.48%	84.39%	88.41%
Percent of improvment	-	37.2%	43.8%

At these operating conditions, the optimal groove structure (shown in figure 3) provides the best mixing performance with η=0.88. The optimal groove generates transverse flow and also stretches the interfacial area for mass transfer as shown in figure 9. Typical T-shaped micromixers have mixing index of 64%. For micromixers with obstacles this number stretches to 84%. As given in table 5 the grooved micromixer (the second optimized geometry) provides an 88% of mixing efficiency which is very fulfilling. This outstanding mixing efficiency was a result of its geometric parameters that were chosen carefully to decrease the mixing length and therefore enhance the mixing efficiency. Another reason for this significant change in mixing efficiency was clarified is figure 11. As it is clear convective flux plays a major role in mixing process. While mixing through diffusion still occurs at the interface between the two fluids its contribution to the total mixing represents less than 10 % of the total mixing. It has been delineated that inserting obstacles and grooves would increase the convective flux. Therefore, the optimized geometry, by enhancing the convective flow will result in an improved mixing efficiency, which was the basis of this paper.

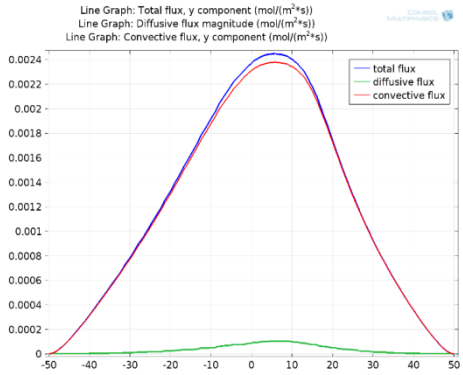

Fig. 11. Demonstration of convective and diffusive flux portion of total flux

4. Conclusion

In this paper a low Reynolds basic T-shaped micromixer was analyzed and compared to two other geometries with obstacles and grooves. This comparison was made conducting COMSOL Multiphysics software. The concentration and velocity distribution in these micromixers was investigated and it was presented that obstacles and grooves enhanced the mixing efficiency by 37.2% and 43.8%, respectively. Also, the contribution of diffusive flux was proven to be insignificant in mixing process. Moreover, it was clarified that this increase in mixing efficiency is due to the development of transversal components of the flow field. As proved, grooved T-shaped micromixer successfully produced enough transverse flow for a satisfactory mixing, which resulted in a desirable mixing efficiency of 88%, and shortest mixing length, which makes it desirable for LOC applications.

References

[1] I. Bernacka - Wojcik et al., Experimental optimization of a passive planar rhombic micromixer with obstacles for effective mixing

in a short channel length, RSC Advances 4 (99) (2014) 56013-56025.

[2] M.S. Virk, A.E. Holdø, Numerical analysis of fluid mixing in T-Type micro mixer, The International Journal of Multiphysics 2 (1) (2008) 107-127.

[3] N.-T. Nguyen, Z. Wu, Micromixers—a review, Journal of Micromechanics and Microengineering 15 (2) (2005) R1-R16.

[4] X.-B. Wang et al., Cell separation by dielectrophoretic field-flow-fractionation. Analytical Chemistry 72 (4) (2000) 832-839.

[5] Y. Shi et al., Radial capillary array electrophoresis microplate and scanner for high-performance nucleic acid analysis, Analytical Chemistry 71 (23) (1999) 5354-5361.

[6] V. Rudyak, A. Minakov, Modeling and Optimization of Y-Type Micromixers, Micromachines 5 (4) (2014) 886-912.

[7] G.S. Jeong et al., Applications of micromixing technology, Analyst 135 (3) (2010) 460-473.

[8] I. Sabotin et al., Optimization of grooved micromixer for microengineering technologies, Informacije MIDEM 43 (2013) 3-13.

[9] Y.Z. Liu, , B.J. Kim, H.J. Sung, Two-fluid mixing in a microchannel, International journal of heat and fluid flow 25 (6) (2004) 986-995.

[10] A. Kumar et al., Effect of geometry of the grooves on the mixing of Fluids in micro mixer channel, in COMSOL Conference (2012).

[11] M. Itomlenskis, P.S. Fodor, M. Kaufman, Design of Passive Micromixers using the COMSOL Multiphysics software package, in Proceedings of COMSOL Conference (2008).

[12] S. Vanka, G. Luo, C. Winkler, Numerical study of scalar mixing in curved channels at low Reynolds numbers, AIChE journal 50 (10) (2004) 2359-2368.

[13] 1. Bernacka-Wojcik et al., Experimental optimization of a passive planar rhombic micromixer with obstacles for effective mixing in a short channel length, RSC Advances 4 (99) (2014) 56013-56025.

[14] J. Aubin, D.F. Fletcher, C. Xuereb, Design of micromixers using CFD modelling, Chemical Engineering Science 60 (8) (2005) 2503-2516.

[15] Y-C. Lin,., Y.-C. Chung, C.-Y. Wu, Mixing enhancement of the passive microfluidic mixer with J-shaped baffles in the tee channel, Biomedical microdevices 9 (2) (2007) 215-221.

[16] D. Gobby, P. Angeli, A. Gavriilidis, Mixing characteristics of T-type microfluidic mixers, Journal of Micromechanics and microengineering,. 11 (2) (2001) 126.

[17] M. Engler et al., Numerical and experimental investigations on liquid mixing in static micromixers. Chemical Engineering Journal 101 (1) (2004) 315-322.

[18] J.-T. Yang, K.-J. Huang, Y.-C. Lin, Geometric effects on fluid mixing in passive grooved micromixers, Lab on a Chip 5 (10) (2005) 1140-1147.

[19] A. Soleymani, , H. Yousefi, I. Turunen, Dimensionless number for identification of flow patterns inside a T-micromixer, Chemical Engineering Science 63 (21) (2008) 5291-5297.

[20] T. Shih, C.-K. Chung, A high-efficiency planar micromixer with convection and diffusion mixing over a wide Reynolds number range, Microfluidics and Nanofluidics 5 (2) (2008) 175-183.

[21] S.S. Ghadge, N. Misal, Design and Analysis of Micro-Mixer for Enhancing Mixing Performance. International Journal of Emerging Trends in Science and Technology 1 (08) (2014) 1342-1346.

[22] A.A.S. Bhagat, , E.T. Peterson, I. Papautsky, A passive planar micromixer with obstructions for mixing at low Reynolds numbers, Journal of micromechanics and microengineering 17 (5) (2007) 1017.

[23] L. Capretto et al, Micromixing within microfluidic devices in Microfluidics, Springer (2011) 27-68.

[24] J.M. Chen, T.-L. Horng, W.Y. Tan, Analysis and measurements of mixing in pressure-driven microchannel flow, Microfluidics and Nanofluidics 2 (6) (2006) 455-469.

[25] R.B. Bird, W.E. Stewart, E.N. Lightfoot, Transport phenomena (1960).

[26] I. Celik, Procedure for estimation and reporting of discretization error in CFD aaplications. ASME Journal of Fluids Engineering 1 (06) (2008).

[27] M. Jain, A. Rao, K. Nandakumar, Numerical study on shape optimization of groove micromixers, Microfluidics and nanofluidics 15 (5) (2013) 689-699.